AAuAl (A = Ca, Sc, and Ti): Peierls Distortion, Atomic Coloring, and Structural Competition

Joyce Pham† and Gordon J. Miller*,†,§

†*Department of Chemistry, Iowa State University, and* §*U.S. Department of Energy, Ames Laboratory, Ames, Iowa 50011–3111, United States*

SUPPORTING INFORMATION

Figure S1. Qualitative phase analysis of the 1Sc: 2Au: 5Al molar loading; ScAuAl atomic coordination spheres in the asymmetric unit of the Fe_2P substructure.

Table S1–S4. Selected crystallographic, atomic coordinates, and displacement parameters of ScAuAl in the Fe_2P substructure (S1 & S3) and Mg_2Ga superstructure (S2 & S4) as selected from the molar loading ratios 1Sc: 2Au: 5Al and 1Sc: 1Au: 1Al, respectively.

Table S5. ScAuAl (Fe_2P) structural coloring models and numbers of selected interatomic distances for atomic site preference analysis.

Table S6–S7. ScAuAl (Fe_2P) and competing structural models total calculated energies, numbers of interatomic interactions at various distances, and formation energies.

Table S8–S9. CaAuAl (TiNiSi-type) and competing structural models total calculated energies, numbers of interatomic interactions at various distances, and formation energies.

Table S10–S11. TiAuAl (Ni_2In-type) and competing structural models total calculated energies, numbers of interatomic interactions at various distances, and formation energies.

Table S12. ScAuAl (Fe_2P) structural parameters before and after VASP optimization as used for subsequent electronic structural calculations and plots.

Table S13. Wigner Seitz radii for Ca, Sc, Ti, Au, and Al atoms as used for subsequent LMTO calculations and plotting of DOS and –COHP curves for pairwise interactions < 3.5 Å.

Figure S2. ScAuAl DOS and COHP curves in competing structures in the $CaIn_2$-type derivatives: NdPtSb, LiGaGe, and ScAuSi. The main text includes electronic structures of ScAuAl in the TiNiSi and Ni_2In structures, which are the most competitive to the experimental model.

Figure S3. CaAuAl DOS and COHP curves for the experimental (TiNiSi-type) and competing structures Fe_2P, Ni_2In, NdPtSb, LiGaGe, and ScAuSi.

Figure S4. TiAuAl DOS and COHP curves for the experimental (Ni_2In-type) and competing structures Fe_2P, TiNiSi, NdPtSb, LiGaGe, and ScAuSi.

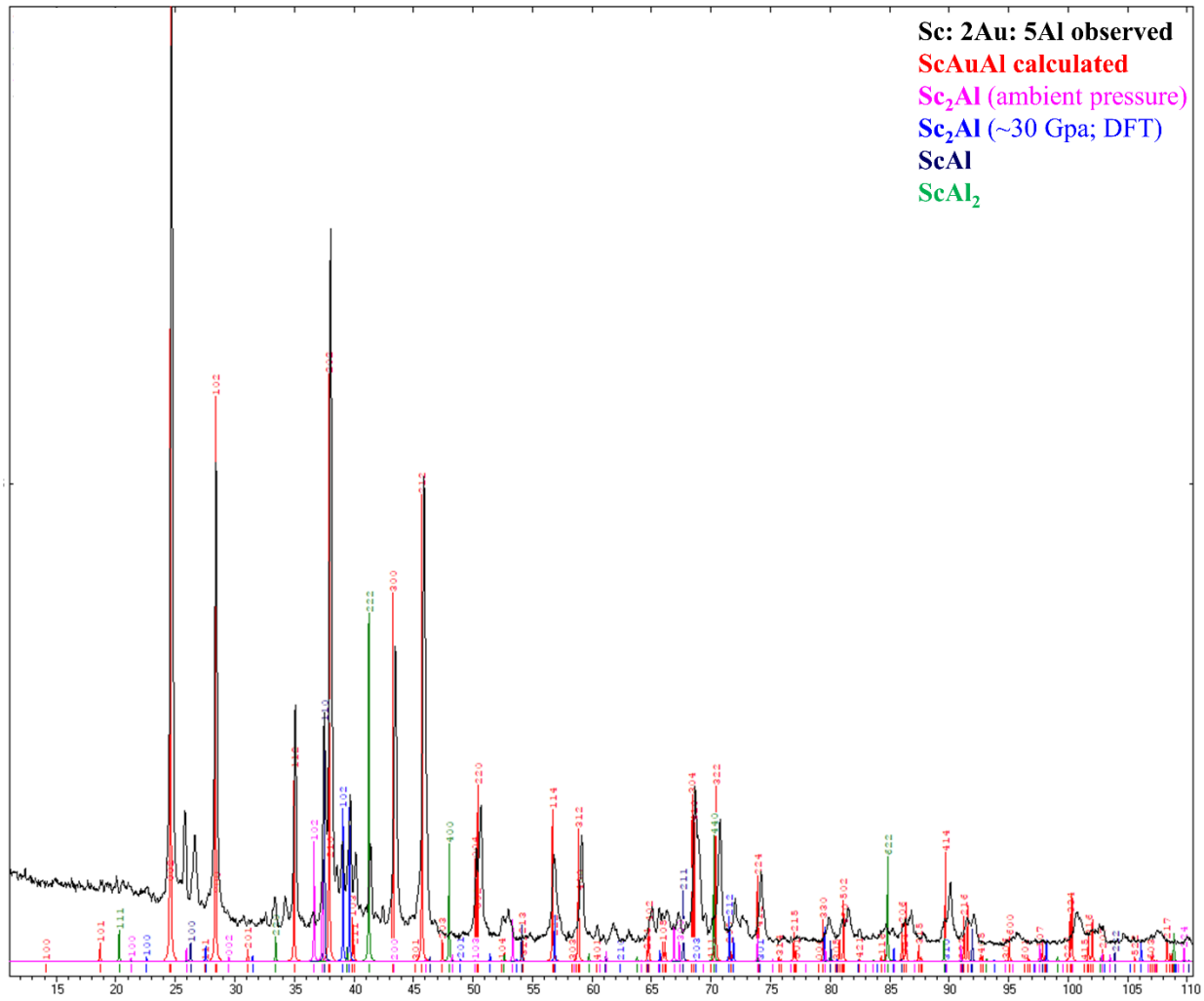

Figure S1A. Phase analysis of the loading 1Sc: 2Au: 5Al showing *probable traces* of at most two of Sc_2Al, ScAl, and $ScAl_2$ with ScAuAl as the major phase.

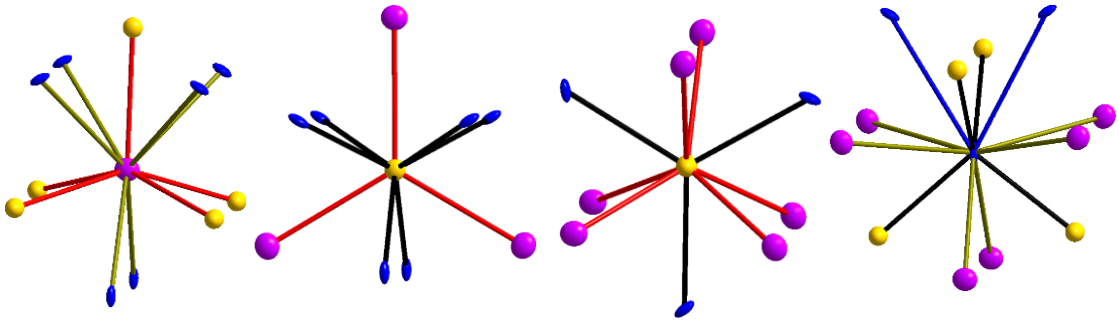

Figure S1B. Coordination spheres of atoms in the asymmetric unit cell of the Fe_2P substructure: {[Au1$(Au2)_2Al_6$]@Sc}, {(Sc_3Al_6)@Au1}, {(Sc_6Al_3)@Au2} and {$(Sc_6(Au1)_2(Au2)_2$. Sc atoms are represented in dark pink, Au atoms are in dark yellow, and Al atoms are in blue.

Table S1. ScAuAl selected refined crystallographic data and structural parameters from loading 1Sc: 2Au: 5Al

instrument	Bruker CCD APEX II											
radiation; λ (Å)/ temp.(K)	Mo Kα; 0.71073/298											
θ range data collection	3.3°–31.4°			3.3°–29.7°			3.3°–31.1°					
absorp. coeff. μ (mm^{-1})/ correction	71.83/ empirical			70.51/ empirical			70.49/ empirical					
meas./ indpnt./ obs. [I > 2σ(I)]/ para.	3879/ 226/ 213/ 15			655/ 184/ 167/ 15			1831/ 223/ 211/ 15					
R[F^2 > 2σ(F^2)]/ wR(F^2)/ R$_{int}$/ GOF	0.016/ 0.040/ 0.032/ 1.21			0.045/ 0.110/ 0.047/ 1.14			0.022/ 0.049/ 0.050/ 1.11					
space group/ Pearson symbol	$P\bar{6}2m$ / *hP*9											
Δρ$_{max}$, Δρ$_{min}$ (e Å^{-3})	1.25, −2.00			4.36, −3.23			1.70, −3.00					
dimensions (Å)	*a* = 7.2067(6) *c* = 3.6217(3)			*a* = 7.219(4) *c* = 3.610(2)			*a* = 7.197(5) *c* = 3.633(2)					
volume (Å^3)/ Z	162.90(2)/ 3			162.9(2)/ 3			163.0(2)/ 3					
index ranges	$-10 \le h, k \le 10$ $-5 \le l \le 5$			$-9 \le h \le 10$ $-7 \le k \le 6$ $-3 \le l \le 5$			$-10 \le h \le 9$ $-10 \le k \le 10$ $-5 \le l \le 5$					
absolute structure parameter	0.02(3)			0.04(7)			0.00(4)					
Au1 (1*a*, $\bar{6}2m$) *x*, *y*, *z*, U$_{iso}$	0, 0, 0		0.0110(2)	0, 0, 0		0.0173(6)	0, 0, 0		0.0054(3)			
Au2 (2*d*, $\bar{6}$..) *x*, *y*, *z*, U$_{iso}$	1/3, 2/3, 1/2		0.0198(2)	1/3, 2/3, 1/2		0.0248(6)	2/3, 1/3, 1/2		0.0139(3)			
Al (3*f*, *m*2*m*) *x*, *y*, *z*, U$_{iso}$	0.2642(5), 0, 1/2		0.0088(6)	0.267(1), 0, 1/2		0.011(1)	0.7371(7), 0, 1/2		0.0053(9)			
Sc (3*g*, *m*2*m*) *x*, *y*, *z*, U$_{iso}$	0.5979(3), 0, 0		0.0157(5)	0.599(1), 0, 0		0.022(1)	0.4023(5), 0, 0		0.0096(7)			
1*a*–1*a* (along *c*), 1*a*–3*f*, 1*a*–3*g* (Å)	3.6217(3)	2.627(1)	2.898(1)	3.610(2)	2.638(5)	2.893(9)	3.633(2)	2.623(2)	2.895(3)			
2*d*–2*d* (along *c*), 2*d*–3*f*, 2*d*–3*g* (Å)	3.6217(3)	2.687(4)	2.8469(6)	3.610(2)	2.680(8)	2.859(5)	3.633(2)	2.689(5)	2.848(1)			
doubled *c* with disordered sites	$P\bar{6}2c$/ *hP*18											
meas./ indpnt./ obs. [I > 2σ(I)]/	7249/ 383/ 229			8726/ 851/ 405			3473/ 377/ 249					
R[F^2 > 2σ(F^2)]/ wR(F^2)/ *R$_{int}$*/ GOF	0.015/ 0.039/ 0.035/ 1.05			0.035/ 0.099/ 0.113/ 0.97			0.023/ 0.068/ 0.052/ 1.19					
Δρ$_{max}$, Δρ$_{min}$ (e Å^{-3})	1.13, −0.96			2.08, −3.85			1.46, −1.81					
dimensions (Å)	*a* = 7.2074(6); *c* = 7.2443(6)			*a* = 7.226(3); *c* = 7.242(4)			*a* = 7.196(5); *c* = 7.266(5)					
volume (Å^3)/ *Z*/ param.	325.90(6)/ 6/ 23			327.5(3)/ 6/ 23			325.9(5)/ 6/ 23					
index ranges	$-10 \le h, k \le 10$; $-5 \le l \le 5$			$-13 \le h, k, l \le 13$			$-10 \le h, k, l \le 10$					
absolute structure parameter	0.00(3)			0.01(4)			0.00(4)					
Au1(2*b*), *x*, *y*, *z*, U$_{iso}$		0, 0, 1/4	0.0092(2)		0, 0, 1/4	0.0098(2)		0, 0, 1/4	0.0053(3)			
Au2(4*f*), occ., *x*, *y*, *z*, U$_{iso}$	0.54(2)	1/3, 2/3, 0.0195(9)	0.0100(5)	0.55(2)	1/3, 2/3, 0.019(1)	0.0101(4)	0.55(2)	1/3, 2/3, 0.019(1)	0.0050(8)			
Au3(4*f*), occ., *x*, *y*, *z*, U$_{iso}$	0.42(2)	2/3, 1/3, 0.0214(9)	0.0100(5)	0.45(2)	2/3, 1/3, 0.0204(1)	0.0101(4)	0.45(2)	2/3, 1/3, 0.0217(9)	0.0050(8)			
Al/Au(6*g*), occ. *x*, *y*, *z*, U$_{iso}$	0.984/0.16(3)	0.2645(5), 0, 0	0.012(1)	0.981/0.019(4)	0.2649(6), 0, 0	0.010(1)	0.998/0.002(5)	0.2628(8), 0, 0	0.005(2)			
Sc(6*h*), *x*, *y*, *z*, *U$_{iso}$*	0.4019(7), 0.4024(7), 1/4		0.0137(4)	0.401(1), 0.402(1), 1/4		0.0131(5)	0.4040(7), 0.4009(7), 1/4		0.0087(7)			
2*b*–2*b* (*c*-axis), 2*b*–6*g*, 2*b*–6*h*	3.6221(3)	2.629(1)	2.899(6)	3.621(2)	2.635(3)	2.903(8)	3.633(3)	2.622(2)	2.896(6)			
4*f*–4*f* (*c*-axis), 4*f*–6*g*, 4*f*–6*h*	3.312(9), 3.905(9)	2.689(2)	2.753(5), 2.942(6)	3.34(1), 3.90(1)	2.694(5)	2.764(7), 2.842(8)	3.318(9), 3.92(1)	2.693(6)	2.273(5), 2.928(6)			

Table S2. ScAuAl selected refined crystallographic data and structural parameters from loading 1Sc: 1Au: 1Al

instrument	Bruker CCD APEX II								
radiation; λ (Å)/ temp.(K)	Mo Kα; 0.71073/298								
θ range data collection	3.3°–29.0°			3.3°–29.0°			3.3°–29.2°		
absorp. coeff. μ (mm^{-1})/ correction	34.96/ empirical			34.90/ empirical			35.08/ empirical		
meas./ indpnt./ obs. [I > 2σ(I)]/ para.	4550/ 307/ 291/ 19			2725/ 303/ 301/ 19			5164/ 316/ 296/ 19		
R[F^2 > 2σ(F^2)]/ wR(F^2)/ R$_{int}$/ GOF	0.018/ 0.036/ 0.035/ 1.15			0.016/ 0.038/ 0.033/ 1.13			0.022/ 0.054/ 0.061/ 1.10		
space group/ Pearson symbol	$P\bar{6}2c$/ *hP*18								
Δρ$_{max}$, Δρ$_{min}$ (e Å^{-3})	1.35, −1.33			1.52, −1.72			2.26, −2.00		
dimensions (Å)	*a* = 7.2362(10) *c* = 7.2448(10)			*a* = 7.234(3) *c* = 7.263(3)			*a* = 7.2224(2) *c* = 7.2487(3)		
volume (Å^3)/ Z	328.53(10)/ 3			329.2(3)/ 3			327.46(2)/ 3		
index ranges	$-9 \le h, k, l \le 9$			$-9 \le h, k, l \le 9$			$-10 \le h, k, l \le 9$		
absolute structure parameter	0.03(3)			0.03(3)			0.07(4)		
Au1 (2*b*, $\bar{6}$..) *x*, *y*, *z*, U$_{iso}$	0, 0, 1/4		0.0077(2)	0, 0, 1/4		0.0052(2)	0, 0, 1/4		0.0068(3)
Au2 (4*f*, 3..) *x*, *y*, *z*, U$_{iso}$	1/3, 2/3, 0.02100(6)		0.0079(2)	1/3, 2/3, 0.02139(6)		0.0058(2)	1/3, 2/3, 0.02013		0.0082(3)
Al (6*g*, .2.) *x*, *y*, *z*, U$_{iso}$	0.2628(6), 0, 0		0.0080(7)	0.2616(5), 0, 0		0.0064(7)	0.2623(7), 0, 0		0.0042(9)
Sc (6*h*, *m*..) *x*, *y*, *z*, U$_{iso}$	0.4096(4), 0.3947(4), 1/4		0.0075(5)	0.4101(3), 0.3950(4), 1/4		0.0060(4)	0.4092(5), 0.395(5), 1/4		0.0047(6)
2*b*–2*b* (along *c*), 2*b*–6*g*, 2*b*–6*h* (Å)	3.6224(5)	2.626(2)	2.912(3)	3.632(2)	2.623(3)	2.914(3)	3.6244(1)	2.622(2)	2.907(4)
4*f*–4*f* (along *c*), 4*f*–6*g*, 4*f*–6*h* (Å)	3.3181(8), 3.9267(8)	2.708(2)	2.831(2), 2.887(2)	3.321(2), 3.942(2)	2.713(4)	2.832(2), 2.891(2)	3.3325(8) 3.9162(8)	2.705(2)	2.826(4), 2.886(3)

Table S3. Fractional atomic coordinates and displacement parameters of ScAuAl in the Fe_2P substructure as selected from 1Sc:2Au:5Al.

	atom	*wyck*	sym	*x*	*y*	*z*	U_{iso}/U_{eq}	U_{11}	U_{22}	U_{33}	U_{12}	U_{13}	U_{23}
ScAuAl	Au1	1*a*	$\bar{6}2m$	0	0	0	0.0110 (2)	0.0102 (2)	0.0102 (2)	0.0126 (3)	0.0051 (1)	0.000	0.000
	Au2	2*d*	$\bar{6}$..	1/3	2/3	1/2	0.0198 (2)	0.0094 (2)	0.0094 (2)	0.0406 (3)	0.00472 (9)	0.000	0.000
	Al	3*f*	*m*2*m*	0.2642 (5)	0	1/2	0.0088 (6)	0.008 (10)	0.007 (2)	0.011 (1)	0.0037 (7)	0.000	0.000
	Sc	3*g*	*m*2*m*	0.5979 (3)	0	0	0.0157 (5)	0.0166 (8)	0.022 (1)	0.0105 (8)	0.0108 (6)	0.000	0.000
ScAuAl	Au1	1*a*	$\bar{6}2m$	0	0	0	0.0173 (6)	0.0181 (9)	0.0181 (9)	0.016 (1)	0.0090 (4)	0.000	0.000
	Au2	2*d*	$\bar{6}$..	1/3	2/3	1/2	0.0248 (6)	0.0172 (8)	0.0172 (8)	0.040 (1)	0.0086 (4)	0.000	0.000
	Al	3*f*	*m*2*m*	0.267 (1)	0	1/2	0.011 (1)	0.017 (4)	0.004 (5)	0.009 (4)	0.002 (2)	0.000	0.000
	Sc	3*g*	*m*2*m*	0.599 (1)	0	0	0.022 (1)	0.026 (3)	0.029 (5)	0.013 (3)	0.015 (2)	0.000	0.000
ScAuAl	Au1	1*a*	$\bar{6}2m$	0	0	0	0.0054 (3)	0.0062 (3)	0.0062 (3)	0.0039 (4)	0.0031 (2)	0.000	0.000
	Au2	2*d*	$\bar{6}$..	2/3	1/3	1/2	0.0139 (3)	0.0051 (3)	0.0051 (3)	0.0315 (5)	0.0026 (2)	0.000	0.000
	Al	3*f*	*m*2*m*	0.7371 (7)	0	1/2	0.0053 (9)	0.006 (2)	0.004 (2)	0.005 (2)	0.002 (1)	0.000	0.000
	Sc	3*g*	*m*2*m*	0.4023 (5)	0	0	0.0096 (7)	0.013 (1)	0.014 (2)	0.002 (1)	0.0072 (8)	0.000	0.000

Table S4. Fractional atomic coordinates and displacement parameters of ScAuAl in the Mg_2Ga superstructure as selected from 1Sc:1Au:1Al

	atom	*wyck*	sym	*x*	*y*	*z*	U_{iso}/U_{eq}	U_{11}	U_{22}	U_{33}	U_{12}	U_{13}	U_{23}
ScAuAl	Au1	2*b*	$\bar{6}$..	0	0	1/4	0.0077 (2)	0.0062 (2)	0.0062 (2)	0.0106 (4)	0.0031 (1)	0.000	0.000
	Au2	4*f*	3..	1/3	2/3	0.02100 (6)	0.0079 (2)	0.0058 (2)	0.0058 (2)	0.0121 (3)	0.00291 (10)	0.000	0.000
	Al	6*g*	.2.	0.2628 (6)	0	0	0.0080 (7)	0.008 (1)	0.005 (2)	0.010 (2)	0.0025 (10)	–.0005 (7)	–.0001 (1)
	Sc	6*h*	*m*..	0.4096 (4)	0	1/4	0.0075 (5)	0.008 (1)	0.006 (2)	0.009 (1)	0.004 (1)	0.000	0.000
ScAuAl	Au1	2*b*	$\bar{6}$..	0	0	1/4	0.0052 (2)	0.0035 (2)	0.0035 (2)	0.0088 (3)	0.0017 (1)	0.000	0.000
	Au2	4*f*	3..	1/3	2/3	0.02139 (6)	0.0058 (2)	0.0032 (2)	0.0032 (2)	0.0109 (3)	0.0016 (1)	0.000	0.000
	Al	6*g*	.2.	0.2628 (6)	0	0	0.0064 (7)	0.005 (1)	0.003 (2)	0.011 (2)	0.0014 (9)	–.0008 (6)	–.002 (1)
	Sc	6*h*	*m*..	0.4096 (4)	0	1/4	0.0060 (4)	0.0049 (10)	0.0035 (10)	0.0083 (10)	0.0010 (10)	0.000	0.000
ScAuAl	Au1	2*b*	$\bar{6}$..	0	0	1/4	0.0068 (3)	0.0047 (3)	0.0047 (3)	0.0110 (4)	0.0023 (2)	0.000	0.000
	Au2	4*f*	3..	1/3	2/3	0.02013 (8)	0.0082 (3)	0.0043 (3)	0.0043 (3)	0.0159 (4)	0.0022 (1)	0.000	0.000
	Al	6*g*	.2.	0.2628 (6)	0	0	0.0042 (9)	0.002 (2)	0.004 (2)	0.007 (2)	0.002 (1)	–.0007 (9)	–.002 (2)
	Sc	6*h*	*m*..	0.4096 (4)	0	1/4	0.0047 (6)	0.003 (1)	–.001 (1)	0.009 (1)	–.003 (1)	0.000	0.000

Table S5. ScAuAl (Fe_2P substructure) coloring models and frequencies of atomic interactions

distance (Å)	**Experimental** 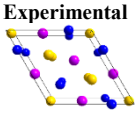	**α** 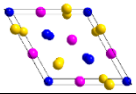	**β** 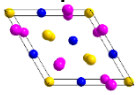	**γ** 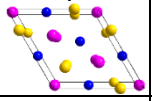	**δ** 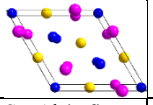	**ε** 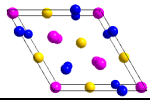
2.638(5)	Au–Al (×6)	Au–Al (×6)	Sc–Au (×6)	Sc–Au (×6)	Sc–Al (×6)	Sc–Al (×6)
2.681(1)	Au–Al (×6)	Au–Al (×6)	Sc–Au (×6)	Sc–Au (×6)	Sc–Al (×6)	Sc–Al (×6)
2.848(5)	Sc–Au (×12)	Sc–Al (×12)	Au–Al (×12)	Sc–Al (×12)	Au–Al (×12)	Sc–Au (×12)
2.893(5)	Sc–Au (×3)	Sc–Al (×3)	Au–Al (×3)	Sc–Al (×3)	Au–Al (×3)	Sc–Au (×3)
3.005(6)	Sc–Al (×6)	Sc–Au (×6)	Sc–Al (×6)	Au–Al (×6)	Sc–Au (×6)	Au–Al (×6)
3.125(3)	Sc–Al (×12)	Sc–Au (×12)	Sc–Al (×12)	Au–Al (×12)	Sc–Au (×12)	Au–Al (×12)
3.331(2)	Al–Al (×3)	Au–Au (×3)	Sc–Sc (×3)	Au–Au (×3)	Sc–Sc (×3)	Al–Al (×3)
Δ*E* (eV/f.u.)	0	+0.347	+0.960	+1.480	+1.759	+2.112

Table S6. ScAuAl competing structures with calculated total energies and numbers of selected interatomic distances

	Fe_2P (Expt.)	Co_2Si	NdPtSb	LiGaGe	Ni_2In	ScAuSi	Cu_2Sb
eV/f.u.	–15.478	–15.447	–15.401	–15.399	–15.397	–15.338	–14.674
$\Delta E_{rel.}$	0.000	+0.031	+0.077	+0.079	+0.081	+0.140	+0.804
space group	$P\bar{6}2m$	*Pnma*	$P6_3mc$	$P6_3mc$	$P6_3/mmc$	$P\bar{6}m2$	$P4/nmm$
lattice para.							
a	7.287	6.674	4.459	4.459	4.467	4.427	4.242
b		4.378					
c	3.625	7.636	6.419	6.428	6.389	6.623	6.654
Å³/f.u.	55.563	55.779	55.257	55.333	55.191	56.213	59.867
Sc–Au	2.848 (4×)	2.749 (1×)	3.176 (3×)	2.835 (3×)	3.143 (6×)	2.841 (3×)	
	2.893 (1×)	2.764 (2×)	3.329 (3×)	3.231 (3×)		3.107 (3×)	
		2.877 (1×)					
		2.893 (2×)					
Sc–Al	3.005 (2×)	2.571 (2×)	3.132 (3×)	2.850 (3×)	3.143 (6×)	2.797 (3×)	3.486 (4×)
	3.125 (4×)	2.612 (1×)	3.377 (3×)	3.212 (3×)		3.162 (3×)	
		2.633 (2×)					
		3.472 (1×)					
Sc–Sc		3.145 (1×)		3.423 (1×)		3.501 (0.5×)	
		3.216 (1×)					
Au–Al	2.638* (2×)	2.307 (2×)	2.596 (3×)	2.576 (3×)	2.451 (3×)	2.494 (3×)	2.725 (4×)
	2.681 (2×)	2.346 (1×)		2.752* (1×)			
		2.353* (1×)					
Al–Al	3.331 (1×)					2.762 (0.5×)	
Au–Au		2.660(×1)				2.936 (0.5×)	3.217 (2×)

*Interlayer distance crossing *c*-axis if the structure were represented as "layers".

Table S7. ScAuAl competing structures and calculated formation energies

Model	$\Delta E_{reaction}$ (eV/f.u.)	$\Delta E_{relative}$ (eV/f.u.)
Experimental (Fe_2P-type)	−2.308(1)	0.000
TiNiSi	−2.277(1)	+0.031
NdPtSb	−2.231(5)	+0.077
LiGaGe	−2.229(1)	+0.079
Ni_2In	−2.227(1)	+0.081
ScAuSi	−2.169(1)	+0.140
Cu_2Sb-type	−1.504(2)	+0.804

Table S8. CaAuAl competing structures with calculated total energies and numbers of selected interatomic distances

	Fe_2P	Co_2Si (Expt.)	NdPtSb	LiGaGe	Ni_2In	ScAuSi	Cu_2Sb
eV/f.u.	–10.976	–11.114	–10.900	–10.897	–10.897	–10.902	–10.606
$\Delta E_{rel.}$	+0.138	0.000	+0.213	+0.217	+0.216	+0.212	+0.508
space group	$P\bar{6}2m$	*Pnma*	$P6_3mc$	$P6_3mc$	$P6_3/mmc$	$P\bar{6}m2$	$P4/nmm$
lattice para.							
a	7.255	7.337	4.563	4.564	4.548	4.536	4.579
b		4.552					
c	4.310	7.824	7.526	7.513	7.597	7.703	6.896
$Å^3/f.u.$	65.485	65.319	67.836	67.752	68.043	68.642	72.314
Ca–Au	2.848 (×4)	3.061 (×1)	3.176 (×3)	2.835 (×3)	3.143 (×6)	2.841 (×3)	
	2.893 (×1)	3.101 (×2)	3.329 (×3)	3.231 (×3)		3.107 (×3)	
		3.209 (×2)					
Ca–Al	3.005 (×2)	3.18 (×1)	3.132 (×3)	2.850 (×3)	3.143 (×6)	2.797 (×3)	3.486 (×4)
	3.125 (×4)	3.209 (×2)	3.377 (×3)	3.212 (×3)		3.162 (×3)	
		3.416 (×2)					
Ca–Ca				3.423 (×1)		3.401 (×0.5)	
Au–Al	2.638* (×3)	2.666 (×1)	2.596 (×3)	2.576 (×3)	2.596 (×3)	2.596 (×3)	2.596 (×4)
	2.681 (×2)	2.671 (×1)		2.752* (×1)			
		2.687 (×2)					
Al–Al	3.331 (×1)	3.362 (×1)				2.762 (×0.5)	
Au–Au						2.936 (×0.5)	3.217 (×2)

* Interlayer distances crossing the *c*-axis if structure were represented in "layers".

Table S9. CaAuAl competing structures and calculated formation energies

Model	$\Delta E_{reaction}$ (eV/f.u.)	$\Delta E_{relative}$ (eV/f.u.)
CaAuAl (Co_2Si-type)	−2.144(3)	0.000
Fe_2P-type	−2.007(3)	+0.138
TiNiSi	−2.140(3)	+0.004
NdPtSb type	−1.932(3)	+0.213
LiGaGe type	−1.927(3)	+0.217
Ni_2In	−1.928(5)	+0.216
ScAuSi	−1.932(3)	+0.212
Cu_2Sb-type	−1.636(3)	+0.508

Table S10. TiAuAl competing structures with calculated total energies and numbers of selected interatomic distances

	Fe_2P	Co_2Si	NdPtSb	LiGaGe	Ni_2In (Expt.)	ScAuSi	Cu_2Sb
eV/f.u.	–16.174	–16.096	–16.311	–16.306	–16.331	–16.210	–15.562
$\Delta E_{rel.}$	+0.137	+0.234	+0.020	+0.024	0.000	+0.121	+0.769
space group	$P\bar{6}2m$	*Pnma*	$P6_3mc$	$P6_3mc$	$P6_3/mmc$	$P\bar{6}m2$	$P4/nmm$
lattice para.							
a	6.694	6.516	4.365	4.363	4.461	4.395	3.988
b		4.001					
c	3.977	7.747	6.150	6.161	5.740	6.025	6.671
Å³/f.u.	51.435	50.494	50.740	50.788	49.452	50.392	53.060
Ti–Au	2.848 (×4)	2.749 (×1)	3.176 (×3)	2.835 (×3)	2.932 (×6)	2.841 (×3)	
	2.893 (×1)	2.764 (×2)	3.329 (×6)	3.231 (×3)		3.107 (×3)	
		2.877 (×1)					
		2.893 (×2)					
Ti–Al	3.005 (×2)	2.571 (×2)	3.132 (×3)	2.850 (×3)	2.932 (×6)	2.797 (×3)	3.486 (×4)
	3.125 (×4)	2.612 (×1)	3.377 (×3)	3.212 (×3)		3.162 (×3)	
		2.633 (×2)					
		3.472 (×1)					
Ti–Ti		3.145 (×1)		3.423 (×1)	2.915 (×2)	3.401 (×0.5)	
		3.216 (×1)					
Au–Al	2.638* (×2)	2.307 (×2)	2.596 (×3)	2.576 (×3)	2.545 (×3)	2.494 (×3)	2.725 (×4)
	2.681 (×2)	2.346 (×1)		2.752* (×1)			
		2.353* (×1)					
Al–Al	3.331 (×1)					2.762 (×0.5)	
Au–Au		2.660 (×1)				2.936 (×0.5)	3.217 (×2)

* Interlayer distances crossing the *c*-axis if structure were represented in "layers".

Table S11. TiAuAl competing structures and calculated formation energies

Model	**$\Delta E_{reaction}$ (eV/f.u.)**	**$\Delta E_{relative}$ (eV/f.u.)**
TiAuAl (Ni_2In-type)	−1.522(2)	0.000
Fe_2P	−1.365(2)	+0.137
TiNiSi	−1.288(2)	+0.234
NdPtSb	−1.502(2)	+0.020
LiGaGe	−1.498(2)	+0.024
Ni_2In	−1.523(5)	–0.001
ScAuSi	−1.401(2)	+0.121
Cu_2Sb	−0.753(2)	+0.769

Table S12. ScAuAl VASP optimization for electronic calculations

Parameter	Experimental input	Optimization output
a (Å)	7.219	7.2868
b (Å)	7.219	7.2868
c (Å)	3.610	3.6250
V (Å³)	162.93	166.69
Sc (*x*, *y*, *z*)	0.401, 0, 1/2	0.3992, 0, 1/2
Au1 (*x*, *y*, *z*)	0, 0, 1/2	0, 0, 1/2
Au2 (*x*, *y*, *z*)	2/3, 1/3, 0	2/3, 1/3, 0
Al (*x*, *y*, *z*)	0.734, 0, 0	0.73636, 0, 0
Sc–Au1 (3*g*–1*a*) (Å)	2.893	2.909
Sc–Au2 (3*g*–2*d*) (Å)	2.849	2.872
Sc–Al (3*g*–3*f*) (Å)	3.005	3.138 and 3.053
Au1–Al (1*a*–3*f*) (Å)	2.638	2.641
Au2–Al (2*d*–3*f*) (Å)	2.681	2.719
Al–Al (3*f*–3*f*) (Å)	3.331	3.327
E_{tot} (eV/f.u.)	−15.465	−15.478

Table S13. Wigner-Seitz radii for LMTO calculations

Model	**$R_{w.s.}$ (Å)**		
Fe_2P	Sc: 3.317	Ca: 3.287	Ti: 3.311
	Au1: 2.980	Au1: 2.963	Au1: 2.981
	Au2: 3.064	Au2: 3.047	Au2: 3.071
	Al: 2.926	Al: 2.902	Al: 2.927
TiNiSi	Sc: 3.166	Ca: 3.759	Ti: 3.167
	Au: 2.592	Au: 2.942	Au: 2.593
	Al: 2.424	Al: 2.894	Al: 2.423
NdPtSb	Sc: 4.023	Ca: 4.023	Ti: 3.646
	Au: 2.856	Au: 2.856	Au: 2.650
	Al: 2.790	Al: 2.790	Al: 2.496
LiGaGe	Sc: 3.431	Ca: 3.431	Ti: 3.366
	Au: 2.928	Au: 2.928	Au: 2.872
	Al: 2.850	Al: 2.850	Al: 2.786
			E: 1.733
Ni_2In	Sc: 4.000	Ca: 4.000	Ti: 3.699
	Au: 2.650	Au: 2.650	Au: 2.512
	Al: 2.536	Al: 2.503	Al: 2.311
ScAuSi	Sc1: 3.482	Ca1: 3.482	Ti1: 3.482
	Sc2: 3.486	Ca2: 3.476	Ti2: 3.476
	Au: 2.812	Au1: 2.812	Au1: 2.812
	Al: 2.708	Al: 2.708	Al: 2.708

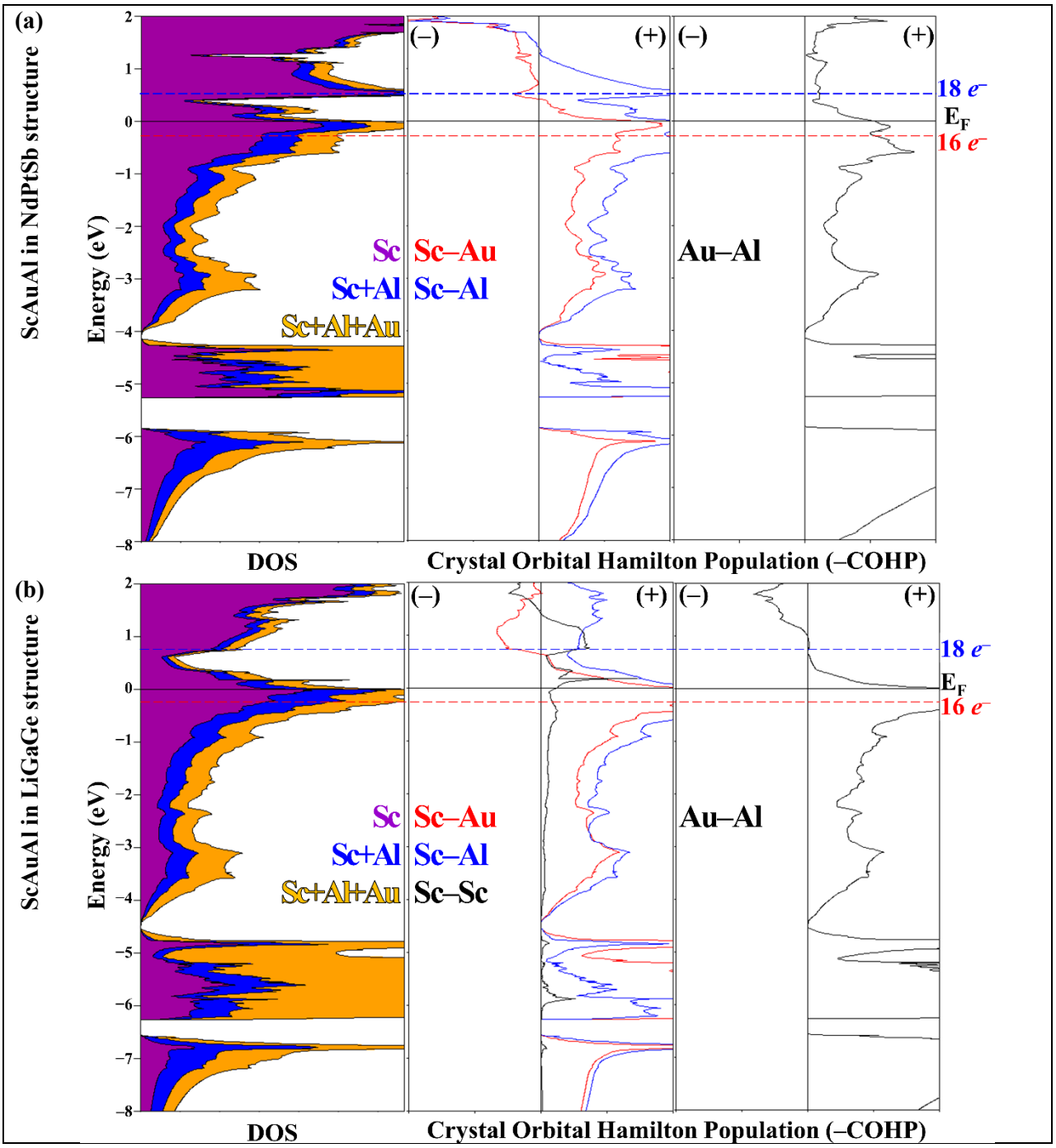
(a)
ScAuAl in NdPtSb structure
Energy (eV)
Sc
Sc+Al
Sc+Al+Au
(–)
(+)
Sc–Au
Sc–Al
Au–Al
18 e⁻
E_F
16 e⁻
DOS
Crystal Orbital Hamilton Population (–COHP)
(b)
ScAuAl in LiGaGe structure
Energy (eV)
Sc
Sc+Al
Sc+Al+Au
Sc–Au
Sc–Al
Sc–Sc
Au–Al
18 e⁻
E_F
16 e⁻
DOS
Crystal Orbital Hamilton Population (–COHP)

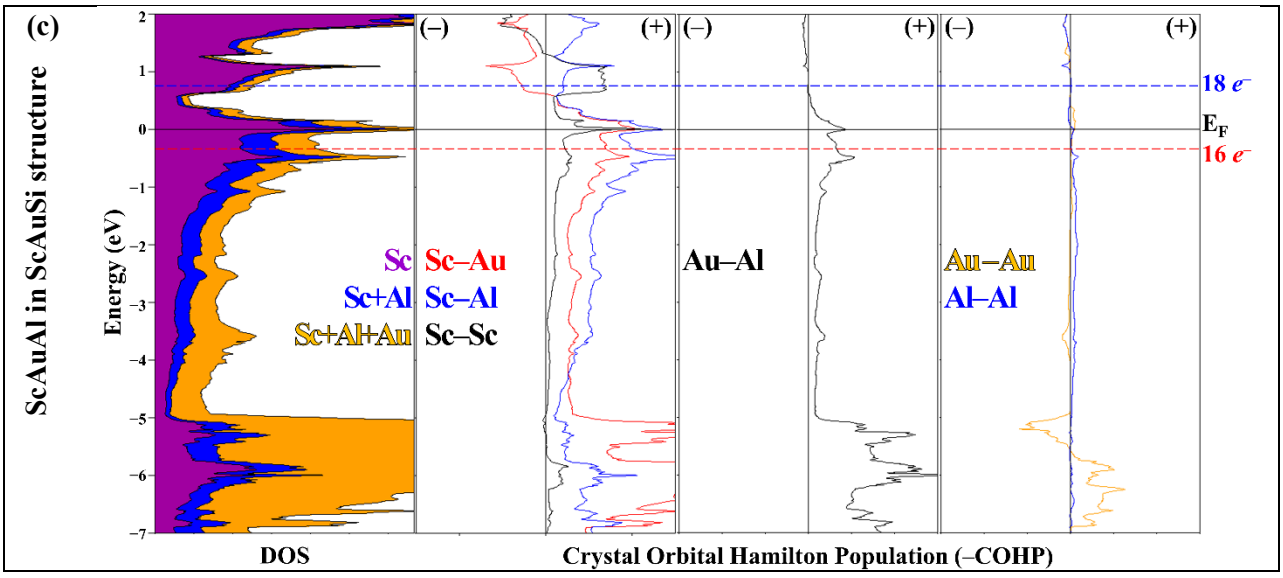

Figure S2. ScAuAl electronic structures in competing structures (a) NdPtSb (b) LiGaGe, and (c) ScAuSi, for all COHP interactions < 3.5 Å and (–) & (+) indicate antibonding and bonding, respectively.

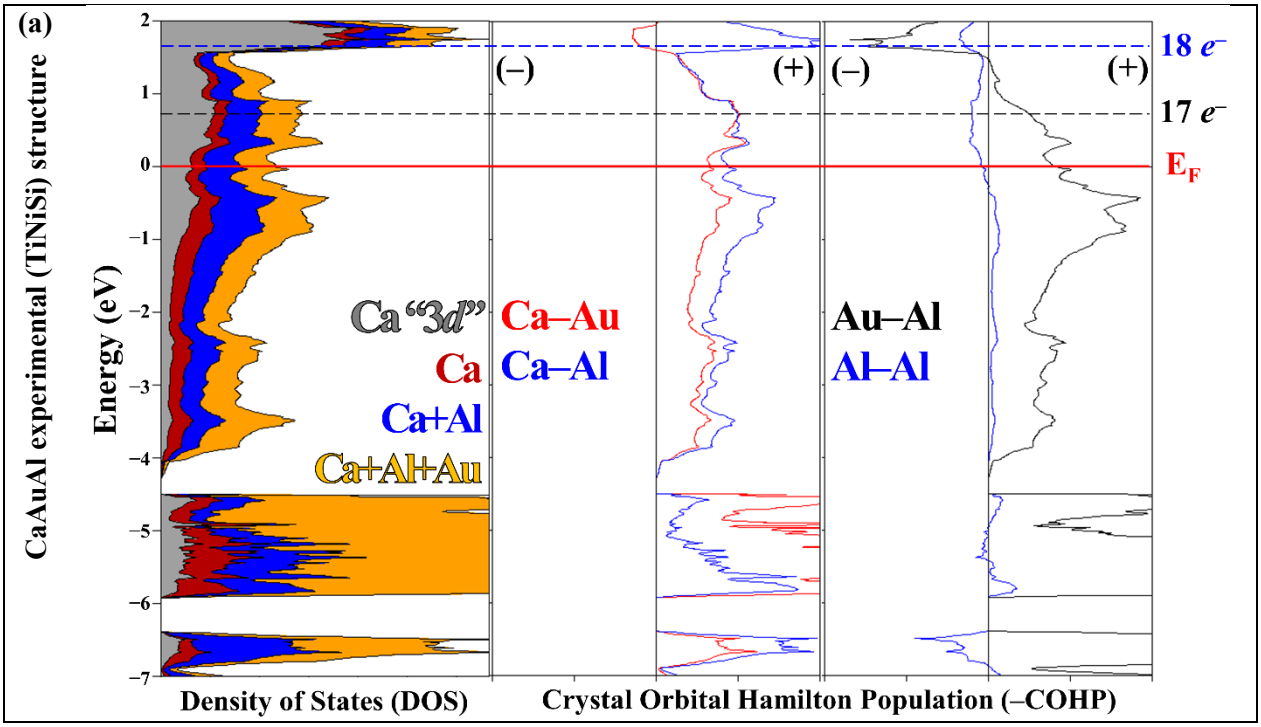

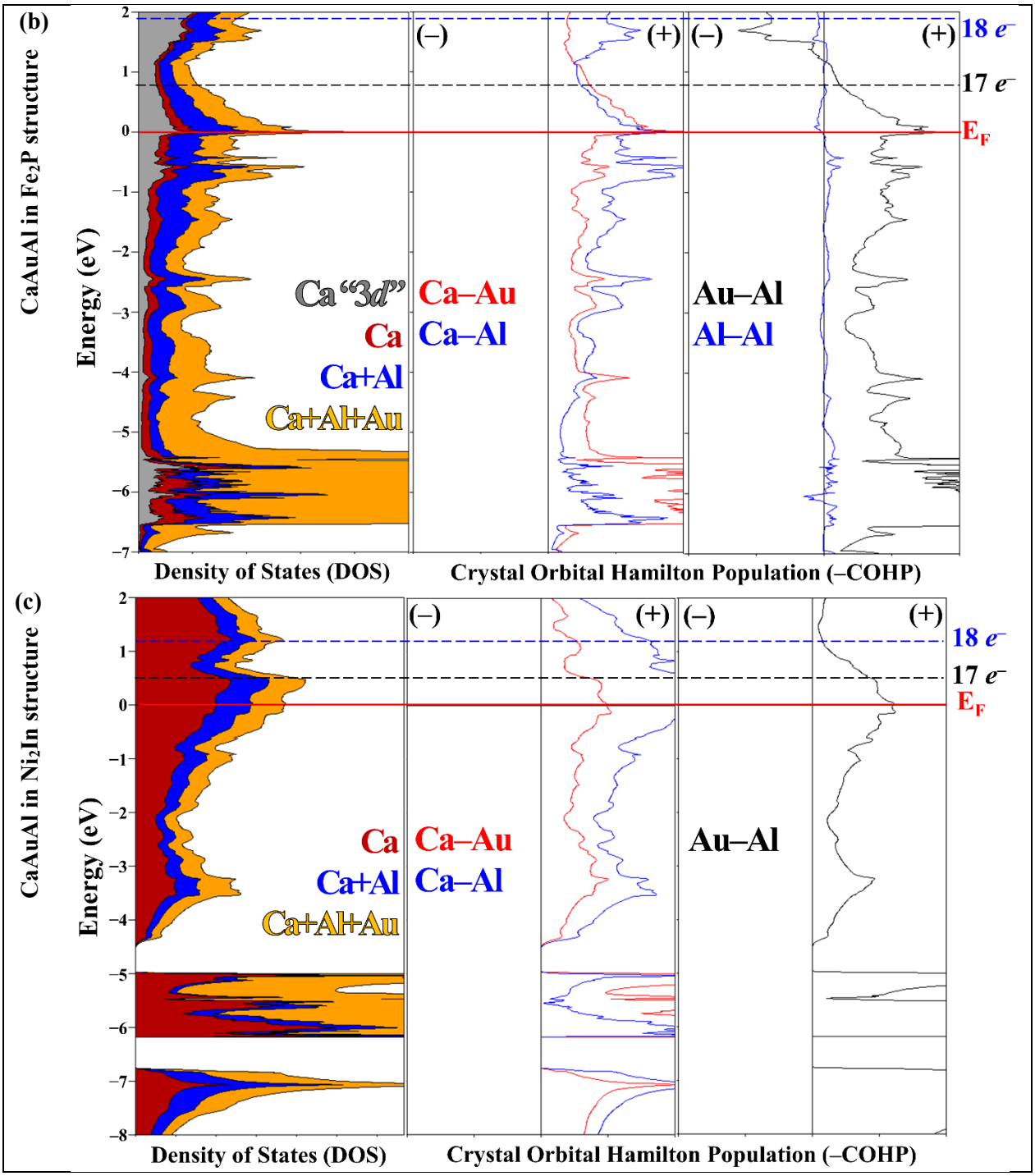
(b)
CaAuAl in Fe2P structure
Energy (eV)
Ca "3d"
Ca
Ca+Al
Ca+Al+Au
Ca–Au
Ca–Al
Au–Al
Al–Al
(–)
(+)
18 e⁻
17 e⁻
EF
Density of States (DOS)
Crystal Orbital Hamilton Population (–COHP)
(c)
CaAuAl in Ni2In structure
Energy (eV)
Ca
Ca+Al
Ca+Al+Au
Ca–Au
Ca–Al
Au–Al
(–)
(+)
18 e⁻
17 e⁻
EF
Density of States (DOS)
Crystal Orbital Hamilton Population (–COHP)

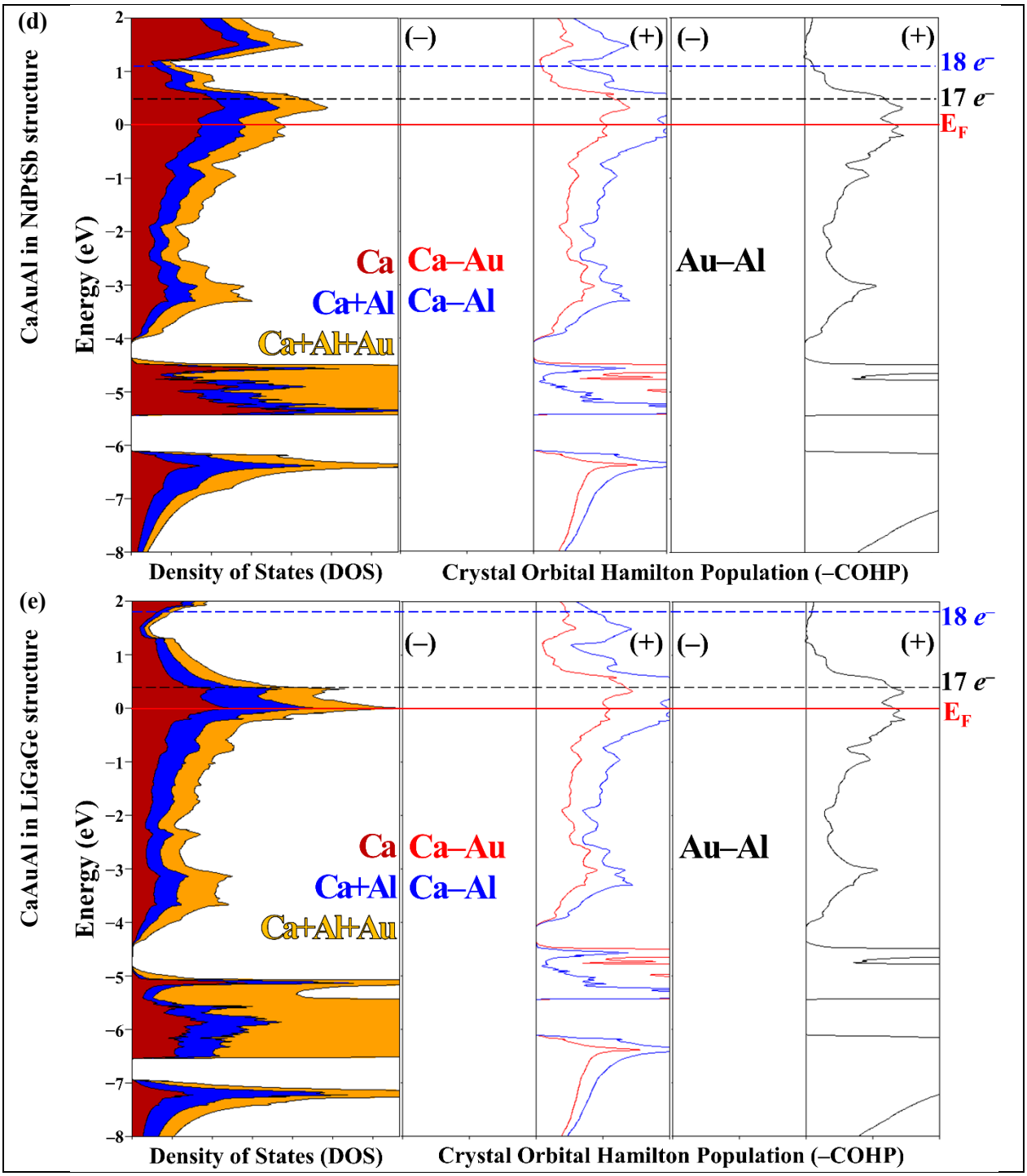
(d)
CaAuAl in NdPtSb structure
Energy (eV)
Ca
Ca+Al
Ca+Al+Au
Ca–Au
Ca–Al
Au–Al
(–)
(+)
18 e⁻
17 e⁻
E_F
Density of States (DOS)
Crystal Orbital Hamilton Population (–COHP)
(e)
CaAuAl in LiGaGe structure
Energy (eV)
Ca
Ca+Al
Ca+Al+Au
Ca–Au
Ca–Al
Au–Al
(–)
(+)
18 e⁻
17 e⁻
E_F
Density of States (DOS)
Crystal Orbital Hamilton Population (–COHP)

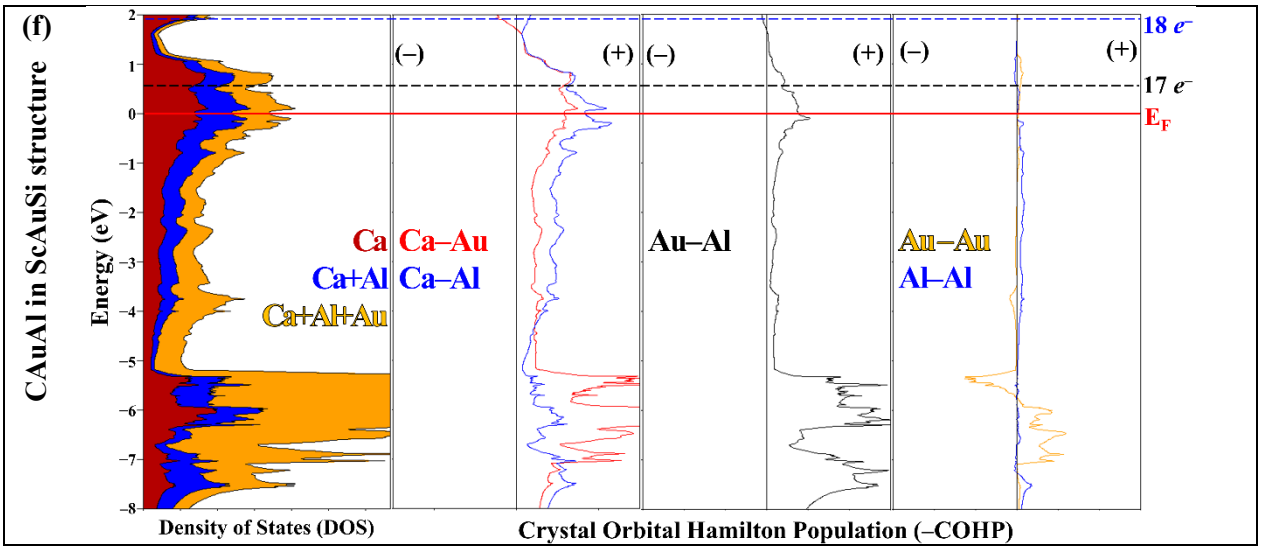

Figure S3. CaAuAl electronic structures (a) and in competing structures (b) Fe_2P (c) Ni_2In, (d) NdPtSb, (e) LiGaGe, and (f) ScAuSi, for all COHP interactions < 3.5 Å and (–) & (+) indicate antibonding and bonding, respectively.

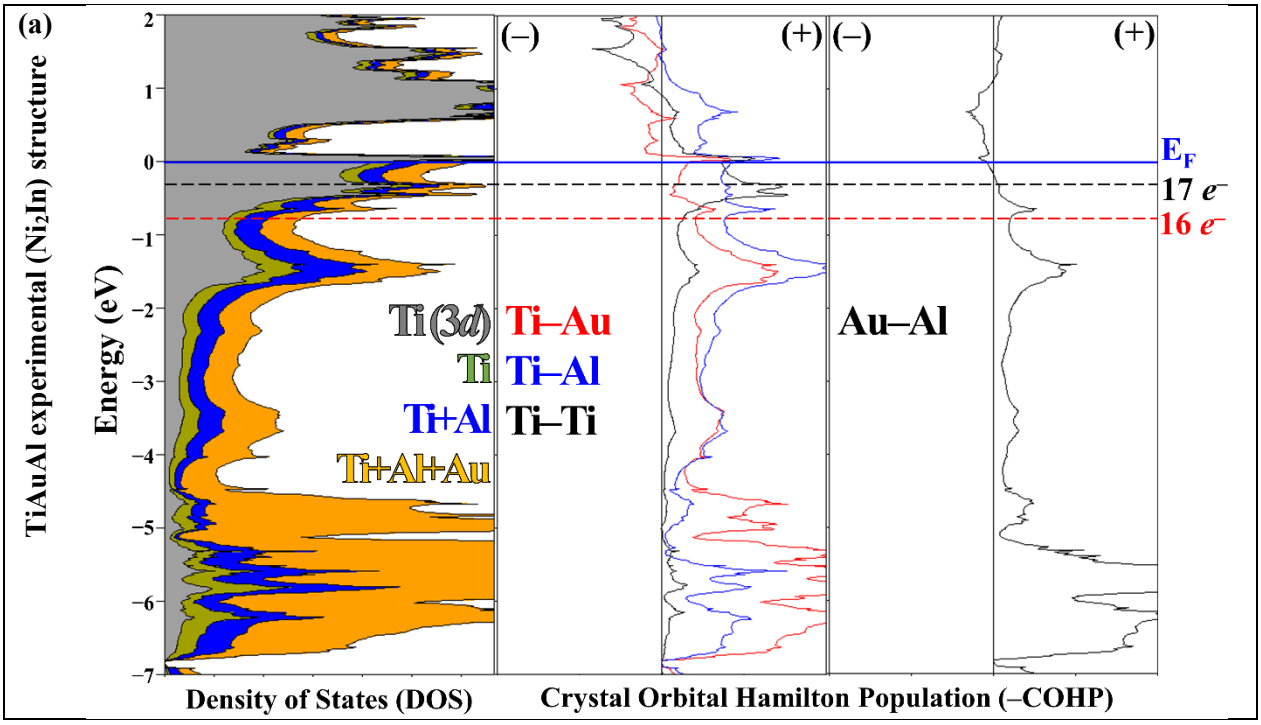

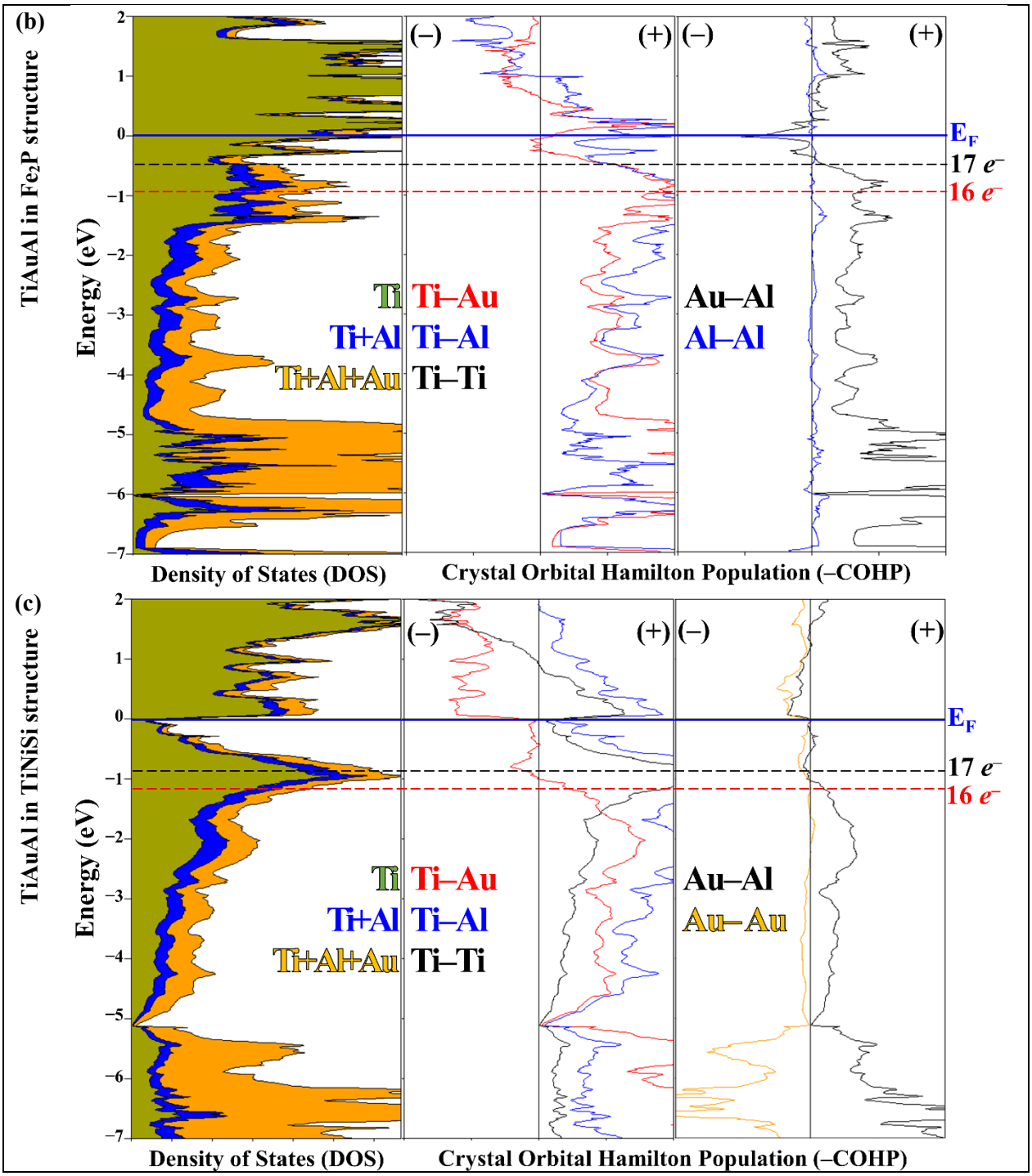
(b)
TiAuAl in Fe2P structure
Energy (eV)
Density of States (DOS)
Crystal Orbital Hamilton Population (–COHP)
(–)
(+)
Ti
Ti+Al
Ti+Al+Au
Ti–Au
Ti–Al
Ti–Ti
Au–Al
Al–Al
EF
17 e–
16 e–
(c)
TiAuAl in TiNiSi structure
Energy (eV)
Density of States (DOS)
Crystal Orbital Hamilton Population (–COHP)
Ti
Ti+Al
Ti+Al+Au
Ti–Au
Ti–Al
Ti–Ti
Au–Al
Au–Au
EF
17 e–
16 e–

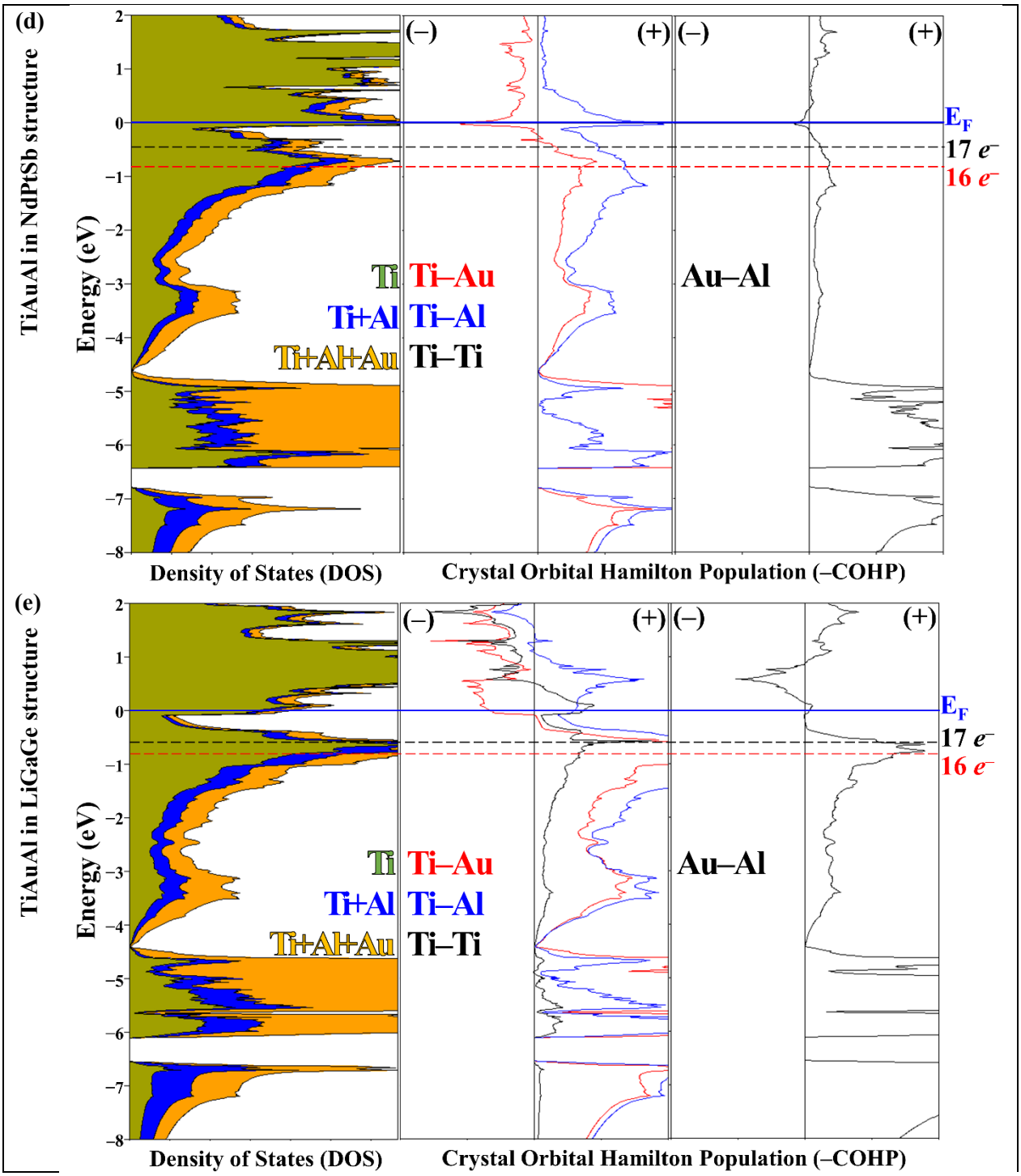
(d)
TiAuAl in NdPtSb structure
Energy (eV)
Ti
Ti+Al
Ti+Al+Au
Ti–Au
Ti–Al
Ti–Ti
Au–Al
(–)
(+)
(–)
(+)
E_F
17 e⁻
16 e⁻
Density of States (DOS)
Crystal Orbital Hamilton Population (–COHP)
(e)
TiAuAl in LiGaGe structure
Energy (eV)
Ti
Ti+Al
Ti+Al+Au
Ti–Au
Ti–Al
Ti–Ti
Au–Al
(–)
(+)
(–)
(+)
E_F
17 e⁻
16 e⁻
Density of States (DOS)
Crystal Orbital Hamilton Population (–COHP)

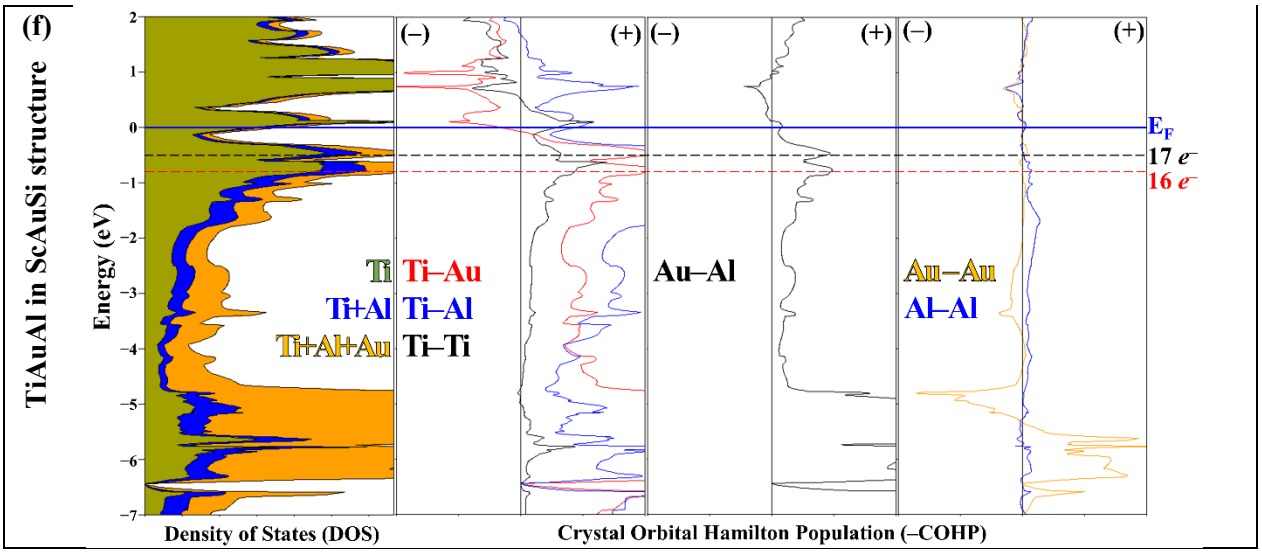

Figure S4. TiAuAl electronic structures (a) and competing structures (b) Fe_2P (c) TiNiSi, (d) NdPtSb, (e) LiGaGe, and (f) ScAuSi, for all COHP interactions < 3.5 Å and (–) & (+) indicate antibonding and bonding, respectively.